3D structure of the CD26–ADA complex obtained by cryo-EM and single particle analysis ☆

Kai Ludwig,[a,1] Hua Fan,[b,1] Jörg Dobers,[b] Markus Berger,[b] Werner Reutter,[b] and Christoph Böttcher[a,*]

[a] *Forschungszentrum für Elektronenmikroskopie, Freie Universität Berlin, Fabeckstr. 36a, D14195, Berlin-Dahlem, Germany*
[b] *Institut für Molekularbiologie und Biochemie, Fachbereich Humanmedizin, Freie Universität Berlin, Arnimallee 22, D-14195, Berlin-Dahlem, Germany*

Abstract

The specific binding of adenosine deaminase to the multifunctional membrane glycoprotein dipeptidyl peptidase IV is thought to be immunologically relevant for certain regulatory and co-stimulatory processes. In this study we present the 3D structure of the complete CD26–ADA complex obtained by single particle cryo-EM at 22 Å resolution. ADA binding occurs at the outer edges of the β-propeller of CD26. Docking calculations of available CD26 and ADA crystal data into the obtained EM density map revealed that the ADA-binding site is stretched across CD26 β-propeller blades 4 and 5 involving the outermost distal hydrophobic amino acids L294 and V341 but not T440 and K441 as suggested by antibody binding. Though the docking of the ADA orientation appears less significant due to the lack of distinct surface features, non-ambiguous conclusions can be drawn in the combination with earlier indirect non-imaging methods affirming the crucial role of the ADA α2-helix for binding.
© 2003 Elsevier Inc. All rights reserved.

Keywords: Dipeptidyl peptidase IV; CD26; Adenosine deaminase; Cryo-TEM; 3D-reconstruction; Single particle analysis

The type II plasma membrane protein dipeptidyl peptidase IV (DPPIV; EC 3.4.14.5; synonymous with CD26) is a widely distributed multifunctional membrane protein [1–5] expressed as a non-covalently linked homodimer of 210 kDa at the cell surface in nearly all mammalian tissues. As an exo-peptidase, it cleaves dipeptides from polypeptides (e.g., chemokines, neuropeptides, and hormones), showing a preference for those possessing proline or alanine in the second position from the N-terminus [6–8], while its gelatinase activity shows that it also has an endo-peptidase function [9].

Besides its enzymatic activity CD26 is involved in cell-adhesion [10–12] and acts as a co-stimulator in T-cell activation [13–15]. CD26 interacts with extracellular adenosine deaminase (ADA, EC 3.5.1.1) and with

tyrosine phosphatase CD45, so that it mediates signal transduction, thereby playing a crucial role in immunoregulation [1,16–18].

In this context CD26 was found to be identical to the ADA binding protein (ADAbp) or ADA complexing protein (ADA-CP) [19]. Although CD26 is expressed in almost all examined species, it binds to ADA only in higher mammals [20,21], where this binding occurs without significant interference with the enzymatic activity of the CD26 [21,22]. Due to the fact that extracellular adenosine (the substrate for ADA) inhibits T-cell proliferation, the allocation of ADA at the cell surface by binding to CD26 plays an important role in the regulation of immune activity by reducing the local concentration of adenosine [22]. In addition, binding of ADA to CD26 induces a co-stimulatory response in T-cell activation [17,23,24] and a regulation of epithelia and lymphocyte cell adhesion [25].

Considerable efforts have been made to study the specific binding properties of ADA to CD26. ADA binding to human CD26 is, e.g., inhibited by the HIV-1

---

glycoprotein gp120, which might have significant consequences in the pathogenesis of AIDS [26]. A number of reports give at least indirect evidence for molecular sites potentially involved in ADA–CD26 binding [27–30].

The catalytic site of CD26 has recently been located and two substrate entry sites have been identified, as well as sites of intermolecular interaction. These data, together with the elucidation of the crystal structure of the dimeric human CD26 at 2.5 Å resolution [31], the detection of a tetrameric complex of porcine CD26 at 1.8 Å resolution [32], as well as the determination of the 3D-structure of dimeric rat CD26 at 16 Å by means of single particle cryo-EM [33], have provided an advanced understanding of the different functionalities of CD26.

The present study now provides the first direct description of the 3D organization of the complete CD26-ADA complex at 22 Å resolution determined by the application of 3D-reconstruction techniques to single molecules of cryo-EM data sets. Considering the known X-ray data of bovine ADA [34,35] (which has therefore been used for complexation in this study) and of human CD26 [31], a three-dimensional fitting into the low resolution EM structure can be calculated by the use of dedicated software [36]. This procedure permits a more advanced study of the protein–protein interaction, compared with the rather moderate resolution of the EM-reconstruction alone. The results are discussed in the light of various earlier reports based on indirect methods.

Materials and methods

Expression, purification, and isolation of homogeneous dimeric human CD26 with enzymatic activity. The full-length cDNA of CD26 was cloned from a human kidney cDNA bank and ligated into the multiple cloning site of pFastBacHTc (Gibco-BRL) vector for expression in Sf9 insect cells. Recombinant bacmid-DNA and high-titer baculovirus stock were generated and human CD26 was expressed in Sf9 cells as described earlier [37].

Specific rabbit anti-CD26 IgGs were separated from polyclonal antiserum and covalently coupled to an Affi-Gel 10 column (Bio-Rad). Human CD26 with enzymatic activity was purified from solubilized insect cells by immunoaffinity chromatography as described previously [33]. The protein concentration was assayed using the BCA protein assay reagent kit (Pierce). DPPIV enzymatic activity was determined with Gly-Pro-4-nitroanilide as substrate as described [38].

Binding of CD26 to ADA and analysis of the CD26–ADA complex by gel electrophoresis and Western blot. Elution fractions were concentrated up to 20 mg/ml with Centriplus YM-30 centrifugal filters (Millipore) at 3000g. Concentrated human CD26 was complexed in the presence of excess bovine ADA type VIII (Sigma) in ADA-binding buffer (50 mM Tris/HCl, 500 mM NaCl, pH 8.0) for 2 h at ambient temperature. The binding results were analyzed by gel electrophoresis under non-denaturing conditions and by Western blot as described earlier [38]. Anti-human DPPIV/CD26 serum (1:500 dilution) and anti-ADA mAb (1:2000 dilution, Chemikon) were used for immunostaining; visualization was performed with peroxidase-conjugated pig anti-rabbit or rabbit anti-mouse IgG (Sigma) and chemiluminescence (Figs. 1A–C).
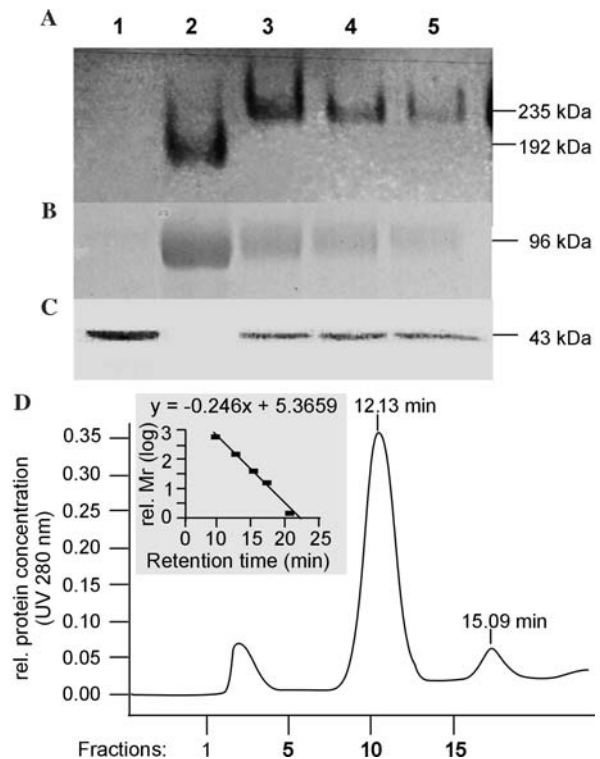

Fig. 1. Analysis and isolation of the CD26–ADA complex. ADA (lane 1) and CD26 (lane 2), binding of CD26 to ADA in ratio 1:0.5 (lane 3), binding of CD26 to ADA in ratio 1:1 (lane 4) and binding of CD26 to ADA in ratio 0.5:1 (lane 5). The binding products were analyzed by non-denaturing PAGE with silver staining (A), Western blot of CD26 using anti-human CD26 sera (1:500 dilution) (B), and Western blot of ADA using anti-ADA mAb (1:2000 dilution) (C). Elution profile of CD26–ADA complex after size exclusion chromatography on a Superdex 200 column (D).

Isolation of CD26 in complex with ADA by size-exclusion fast protein liquid chromatography (SE-FPLC). As much as 100 μl of binding-mixture were loaded on a Superdex 200 column (Pharmacia Biotech), previously equilibrated with 20 mM Tris/HCl, 150 mM NaCl, pH 8.0 and run at a flow rate of 0.5 ml/min with Tris buffer (Fig. 1D). The molecular weight of the eluted protein was determined using thyroglobulin (670 kDa), bovine IgG (158 kDa), myoglobin (44 kDa), cyanocobalamin (17 kDa), and vitamin B12 (1.35 kDa) (all Pharmacia Biotech) as standards. The standard linear regression curve was generated by plotting the log of the molecular mass of different calibration proteins against their retention times (see inset Fig. 1D).

Sample preparation for Cryo-EM. High contrast embedding and vitrification of protein samples were performed as previously described [39].

Cryo-EM. Vitrified samples were transferred into a Tecnai F20 FEG using a Gatan cryoholder and cryostage (Model 626). Imaging was performed at 160 kV accelerating voltage at a defocus value of 600 nm, which corresponds to a first zero of the contrast transfer function at 13 Å (C_s = 2.0 mm). Image recording followed the low-dose protocol of the microscope at a primary magnification of 65,473×.

Image processing. Optical sound micrographs (laser optical check) were digitised using the "Primescan" scanner (Heidelberger Druckmaschinen AG) at a nominal pixel resolution of 0.61 Å in the digitised images. All image-processing procedures were performed with the IMAGIC 5 software (Image Science GmbH). Four thousand five hundred single molecules were interactively selected and classification

as well as "angular reconstitution" techniques were applied [40]. The resolution obtained in the final 3D reconstruction was determined to be ~22 Å according to the 3σ threshold criterion of the Fourier shell correlation [41].

Docking. For docking of crystal data into low-resolution EM density maps, "Situs 2.0" (http://situs.biomachina.org) was used. Corresponding volumes of the complex constituents were extracted by difference mapping followed by "qrange" docking as described in [36].

Results

Preparations of CD26:ADA in molecular ratios of 2:1, 1:1 or 0.5:1, respectively, migrated the same distance through a non-denaturing gel, indicating that preferentially one ADA per CD26 dimer was bound (Fig. 1A). After isolation by size-exclusion fast protein liquid chromatography (SE-FPLC), the CD26–ADA complex (fraction 10) was checked for molecular mass (Fig. 1D) and CD26 enzymatic activity (data not shown).

A first visual inspection of the raw microscopical data of CD26–ADA samples immediately confirmed extra density at least on one of the monomers when compared with preparations of the dimeric CD26 alone. Though the reconstruction of the 3D structure almost instantly revealed the location of the binding site on one of the monomers, a considerably number of CD26 particles were complexed with two molecules of ADA, one on each monomer. This observation is in accordance with reports, which showed that human CD26 could bind two ADA molecules [42–44]. Since this doubly loaded CD26 appears to be less represented in the data set and the spatial binding site was found to be identical for both subunits, we have restricted our presentation to the exact binding location of only the mono-adduct. The corresponding 3D structure of the complex is shown in Fig. 2C as determined from 4500 single particles at a resolution of about 22 Å (3σ threshold).

Typical overall features of the human CD26 structure, which was reported earlier [31] and is represented in Fig. 2A, can be allocated in the reconstruction. Both structures show two identical subunits connected in a typically asymmetric manner, each of them having two separate openings, one at the site, the other in the center of the characteristic β-propeller domain (see
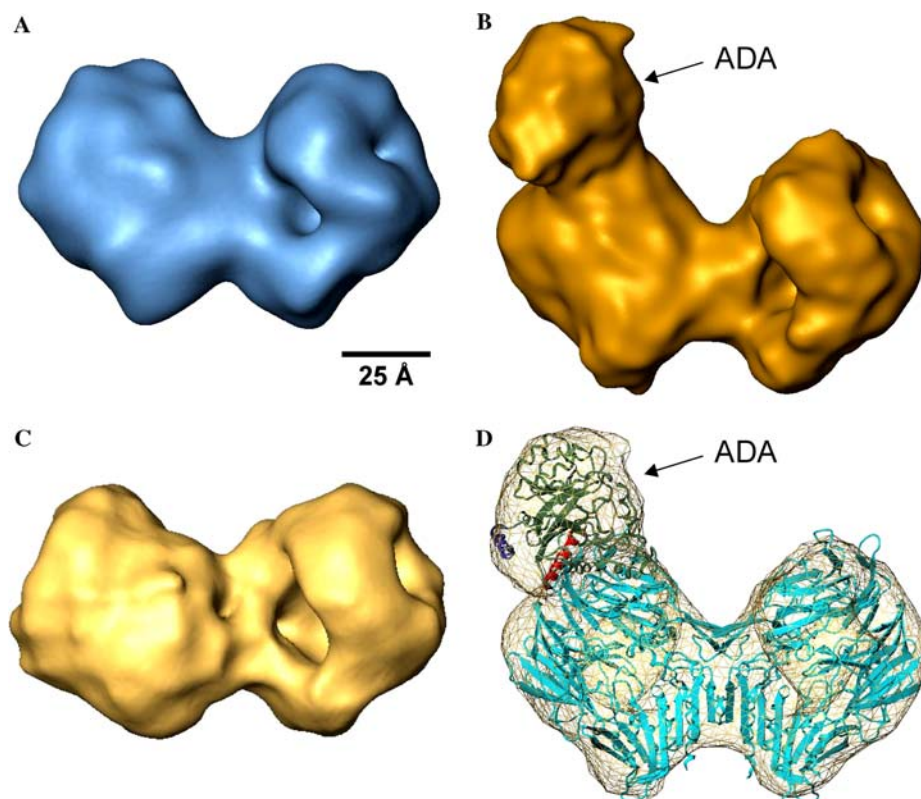

Fig. 2. (A) Surface representation of the crystal structure of human CD26 (1N1M), Gaussian filtered to a resolution, which is comparable to the EM-structure shown in (C). (B) Surface representation of the 3D-reconstruction of rat CD26 at a resolution of 16 Å, previously determined from single particle cryo-EM [33]. (C) Surface representation of the 3D-reconstruction of the human CD26–bovine ADA complex, which was determined from single particle cryo-EM at 22 Å resolution. The 2:1 complex with a single bound ADA molecule is represented here (2:2 complexation, which has also been proven in the data (see text), is not shown). (D) Crystal structures of the human CD26 (1N1M, secondary structure representation, cyan) and of bovine ADA (1KRM, secondary structure representation, green), both of which are docked into the EM density map (C) by the use of "Situs" calculations (yellow mesh surface).

Discussion). The complex of CD26 with ADA (Fig. 2C) reveals additional mass attached to the β-propeller domain of CD26. The rather globular appearance of this extra density is thought to be contributed by the binding of ADA and it agrees with the size and volume expected from the known crystal structure of isolated bovine ADA [45].

Access to both X-ray structures (human CD26 pdb-entry: 1N1M [31]; bovine ADA pdb-entry: 1KRM [45]) should in principle allow a very accurate examination of the binding site, provided that a spatially unambiguous fitting of the structures can be performed. Such docking calculations of the high-resolution crystal data into the low-resolution density map of the EM reconstruction were accomplished by "Situs." The high conformity of both crystal structures with the EM reconstruction was very evident (Fig. 2D). For the CD26 docking, the overall dimensions and geometrical conditions, as well as the structural features like disposition of openings, catalytic domain or propeller domain [31] are perfectly reproduced. Minor differences are detectable for some loop positions, which are not fully enclosed by the 3D-volume.

The docking of the nearly globular ADA appeared more difficult, since this protein lacks very prominent surface features at the achieved moderate resolution of the reconstruction. However, comparing reasonable solutions of the docking calculation (cp. Fig. 4) with earlier results based on the application of various indirect methods [29,30] only one particular orientation of ADA complies with these experimental results (see Discussion).

Discussion

Single particle electron cryomicroscopy was used to reconstruct the 3D-structure of the complete CD26–ADA complex. This 3D-structure clearly shows that ADA binds at the outer edges of the β-propeller of CD26 without any steric interference with the two openings, which are thought to allow direct access to the catalytic site [31–33]. This observation is in agreement with the finding that ADA binding does not affect the enzymatic activity of CD26 [8,21,22,46]. The location of the binding site is in extremely close agreement with the suggestions made by various authors using indirect non-imaging methods [27,28,47]. The relevant aspects in terms of specific CD26-ADA interaction are discussed.

ADA binding site on human CD26

With the availability of the crystal structures of human CD26 and bovine ADA, docking calculations provide direct access to binding patterns on a molecular level. The relevant area for CD26 viewed from two
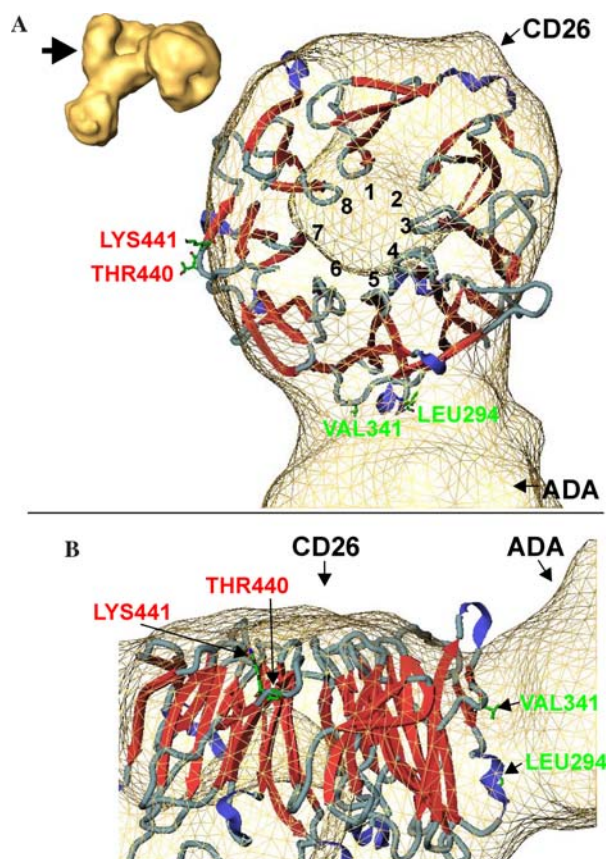

Fig. 3. Area of CD26 ('β-propeller') relevant for ADA binding. The orientation complies with the docking of the crystal structure into the EM density map (yellow mesh surface) by the use of "Situs." (A) Secondary structure representation of the CD26 β-propeller. The viewing angle and the indices are those used by Rassmussen et al. ([31], Fig. 2B). (B) View from (A) tilted out-of-plane by 90° and subsequently rotated clockwise by 90°. See text for details.

different angles (Fig. 3) shows that the ADA-binding is stretched across the β-propeller blades 4 and 5 (residues 282–295 and 322–350).

This result is in good agreement with reports by Dong et al. [22], which authors used sequentially CD26 deletion, human–rat swap and point mutations, and found that the residues of L340, V341, A342, and R343 on the CD26 molecule were essential amino acids for ADA binding. Moreover, the replacement of the peripheral amino acids L294 and V341 (which are not conserved between human and rodent CD26) with hydrophilic residues (L294R and V341K) at either of the two locations decreased ADA binding [28]. This is in impressive accordance with the docking result: As can be seen in the "top view" as well as in the "side view" of the β-propeller (Fig. 3), L294 and V341 are the outermost distal amino acids of the human CD26 at the CD26–ADA interface, providing direct access to the contact region (cp. Fig. 3).

On the other hand, L294 and V341 alone are not sufficient to mediate the binding of ADA, as shown by

the corresponding inverse point mutations of rat CD26. The authors showed that six mAbs found to inhibit ADA binding had an epitope involving residues 340–343 as well as 440–441. This finding suggests that T440/K441 provide additional relevance for ADA binding. However, the docking clearly shows that the residues T440 and K441 are localized outside of the ADA contact region (see Figs. 4A and B, respectively) and are therefore not directly involved in the binding.

Influence of tetramerization of CD26 on ADA binding

Very recently, Engel et al. [32] resolved the crystal structure of CD26 obtained from porcine kidneys at 1.8 Å resolution. Remarkably, the crystal structure revealed a tetrameric assembly, showing two dimers of CD26 to be connected via β-propeller blade 4 of each monomer to form a dimeric dimer complex. The authors supposed i.a. that the tetramerization of CD26 might interfere with the ADA binding. As becomes obvious from our reconstruction and docking calculations, ADA binding would be unambiguously sterically disabled if

CD26 were engaged in a tetrameric arrangement. Tetramerization of CD26 might thus act as a control mechanism for ADA binding. It is noteworth that tetrameric or higher complexes of CD26 have not been found in our preparation.

The CD26 binding site on bovine ADA

Fortunately, the crystal structures of mouse and bovine ADA are known [34,48]. Admittedly, the docking of the crystal structure into the EM density map in the case of bovine ADA is much more critical than for CD26. "Situs" aims at exploiting characteristic features of 3D structures by placing so-called codebook vectors into the density distributions to mark the main features of the protein shape [36]. These vectors provide the information about the shape of the protein relatively unattached from the available resolution and may therefore serve as a set of landmarks for aligning atomic structures to low-resolution data. The CD26 dimer with its very specific geometry allows an unambiguous docking of the crystal structure in the corresponding
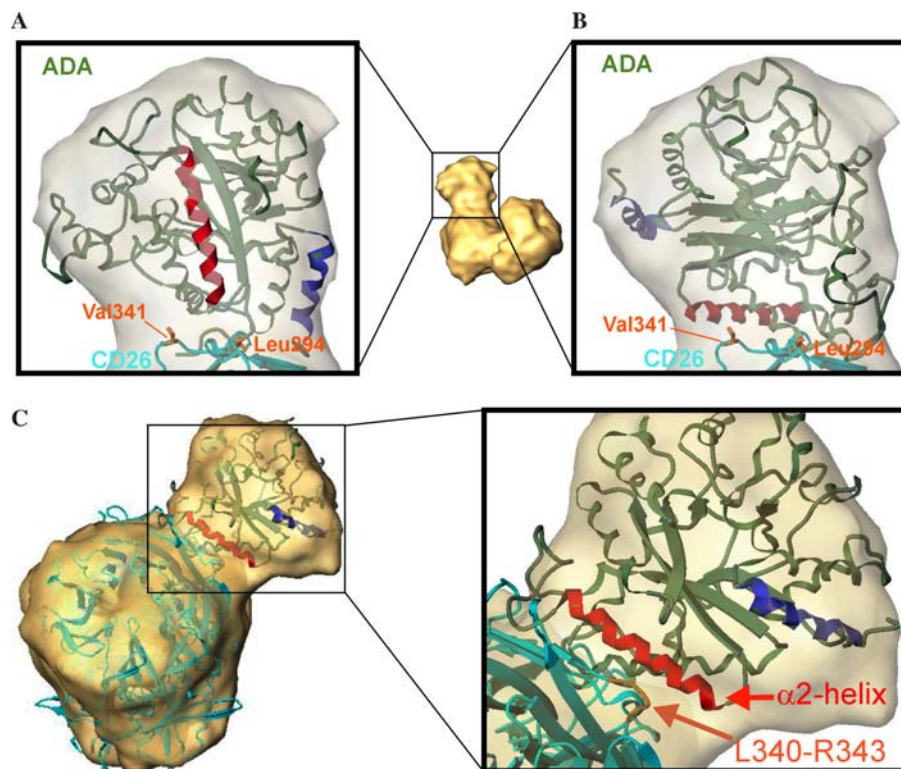

Fig. 4. Crystal structure of bovine ADA (1KRM, secondary structure representation) docked into the EM density map of the CD26–ADA complex as obtained from "Situs" calculations. (A) First, numerically best fitting solution of the ADA docking calculations. The prominent α2 helix is highlighted in red (residues 126–143, see text), the C-terminal helix in blue. Side chain positions of CD26 residues V341 and L294 are also indicated (orange). (B) Alternative (= coincident with indirect experimental data and therefore favored) solution of the ADA docking calculations. Again, the prominent α2 helix is highlighted in red (residues 126–143, see text), the C-terminal helix in blue and the side chains of CD26 residues V341 and L294 in orange. (C) X-ray structure of CD26 (cyan) and ADA (green) docked into the CD26–ADA density map (transparent yellow) by using "Situs" software. Left: view along the longitudinal axis of the CD26 dimer (cell membrane would be located at the bottom). The ADA α2 helix is highlighted in red, the C-terminal helix in blue. Right: close-up view of CD26–ADA complex as indicated. The relevant CD26 loop L340–R343 is highlighted in orange.

EM density map. In case of ADA this alignment is complicated by the protein's almost spherical appearance, which gives rise to only faint surface features at the achieved level of resolution.

The optimum number k of vectors is not known a priori and has to be evaluated by k-dependent criteria. It becomes obvious by looking at the average statistical variability of the codebook vectors that the optimum vector number was $k = 4$ (see Supplementary Material). The three best fits for $k = 4$ (according to the code book vector rmsd [36]) will be discussed below.

According to the first solution the C-terminus (blue helix) of ADA is directly orientated towards the CD26 surface (Fig. 4A). Earlier reports suggested that the C-terminal amino acids L346, A350, and G352 are involved in the CD26 binding by forming a nonconserved hydrophobic region in human ADA, which is predominantly charged in mouse ADA [28]. The latter is not able to bind CD26 of mouse or human, which suggests that this motif is crucial for interaction of ADA with hydrophobic residues of CD26 [27,49]. However, Richard et al. [29] proofed this assumption to be wrong by showing that a human–mouse ADA hybrid (h1–247/m248–352) binds to CD26 in the same manner. Fig. 4A also shows that V341 of CD26 could not come in contact with ADA, but is reportedly involved in ADA binding. We have therefore discarded this particular docking solution.

Solutions two and three of the docking procedure showed both the α2 helix in parallel orientation with respect to the CD26 binding interface. The difference between these two additional options however is marginal, though solution three, which is presented in Fig. 4B, brings the helix in even closer contact to the CD26 binding interface. The α2 helix has been proven to be the keystone in ADA binding. Richard et al. [29,30] demonstrated that the replacement of the entire 18-residue segment of human ADA by the murine equivalent abolished the ADA binding to human and rabbit CD26. As can be seen in the close-up view of Fig. 4C the loop between β-strand 3 and β-strand 4 of the CD26 β-propeller blade 5 which contains the relevant ADA binding residues 340–343 [27] is not only close but nearly parallel orientated to the α2 helix of the ADA. Taken the above arguments together we feel the assumption justified that the third docking solution comprises best all available data and provides a good understanding of its spatial implications.

In conclusion, we can state that although the resolution achieved in our 3D-reconstruction is far too low for the direct assignment of single side chain interactions between the complexed molecules, a significant synergy effect for the examination of even relatively small and asymmetric protein complexes can be achieved by cryo-EM, provided the crystal structures of the constituents are available. The method is suitable for a detailed study

of protein–protein interaction on a level beyond the current attainable resolution of single particle cryo-EM and allows affirming or vitiating conclusions previously derived from indirect non-imaging methods.

References

[1] C. Morimoto, S.F. Schlossman, The structure and function of CD26 in the T-cell immune response, Immunol. Rev. 161 (1998) 55–70.

[2] I. De Meester, S. Korom, J. Van Damme, S. Scharpe, CD26, let it cut or cut it down, Immunol. Today 20 (1999) 367–375.

[3] M.D. Gorrell, V. Gysbers, G.W. McCaughan, CD26: a multifunctional integral membrane and secreted protein of activated lymphocytes, Scand. J. Immunol. 54 (2001) 249–264.

[4] D.J. Drucker, Therapeutic potential of dipeptidyl peptidase IV inhibitors for the treatment of type 2 diabetes, Expert Opin. Investig. Drugs 12 (2003) 87–100.

[5] E. Boonacker, C.J. Van Noorden, The multifunctional or moonlighting protein CD26/DPPIV, Eur. J. Cell. Biol. 82 (2003) 53–73.

[6] R. Mentlein, Dipeptidyl-peptidase IV (CD26): role in the inactivation of regulatory peptides, Regul. Pept. 85 (1999) 9–24.

[7] I. De Meester, C. Durinx, G. Bal, P. Proost, S. Struyf, F. Goossens, K. Augustyns, S. Scharpe, Natural substrates of dipeptidyl peptidase IV, Adv. Exp. Med. Biol. 477 (2000) 67–87.

[8] K. Augustyns, G. Bal, G. Thonus, A. Belyaev, X.M. Zhang, W. Bollaert, A.M. Lambeir, C. Durinx, F. Goossens, A. Haemers, Curr. Med. Chem. 6 (1999) 311–327.

[9] F. Bermpohl, K. Loester, W. Reutter, O. Baum, Rat dipeptidyl peptidase IV (DPP IV) exhibits endopeptidase activity with specificity for denatured fibrillar collagens, FEBS Lett. 428 (1998) 152–156.

[10] W. Reutter, O. Baum, K. Loester, H. Fan, J.P. Bork, K. Bernt, C. Hanski, R. Tauber, Functional aspects of the three extracellular domains of dipeptidyl peptidase IV: characterization of glycosylation events, of the collagen-binding site and endopeptidase activity, in: B. Fleischer (Ed.), Dipeptidyl Peptidase IV (CD26) in Metabolism and the Immune Response, R.G. Landes Company, Texas, 1995, pp. 55–79.

[11] H.C. Cheng, M. Abdel-Ghany, B.U. Pauli, A novel consensus motif in fibronectin mediates dipeptidyl peptidase IV adhesion and metastasis, J. Biol. Chem. 278 (2003) 24600–24607.

[12] W.T. Chen, DPPIV and seprase in cancer invasion and angiogenesis, Adv. Exp. Med. Biol. 524 (2003) 197–203.

[13] B. Fleischer, CD26: a surface protease involved in T-cell activation, Immunol. Today 15 (1994) 180–184.

[14] T. Tanaka, J.S. Duke-Cohan, J. Kameoka, A. Yaron, I. Lee, S.F. Schlossman, C. Morimoto, Enhancement of antigen-induced T-cell proliferation by soluble CD26/dipeptidyl peptidase IV, Proc. Natl. Acad. Sci. USA 91 (1994) 3082–3086.

[15] H. Fan, S. Yan, S. Stehling, D. Marguet, D. Schuppan, W. Reutter, Dipeptidase peptidase IV/CD26 in T cell activation, cytokine secretion and immunoglobulin production, Adv. Exp. Med. Biol. 524 (2003) 165–174.

[16] A. von Bonin, J. Huhn, B. Fleischer, Dipeptidyl-peptidase IV/CD26 on T cells: analysis of an alternative T-cell activation pathway, Immunol. Rev. 161 (1998) 43–53.

[17] R. Franco, A. Valenzuela, C. Lluis, J. Blanco, Immunol. Rev. 161 (1998) 27–42.

[18] S. Yan, D. Marguet, J. Dobers, W. Reutter, H. Fan, Eur. J. Immunol. 33 (2003) 1519–1527.

[19] M.E. Morrison, S. Vijayasaradhi, D. Engelstein, A.P. Albino, A.N. Houghton, A marker for neoplastic progression of human melanocytes is a cell surface ectopeptidase, J. Exp. Med. 177 (1993) 1135–1143.

[20] J. Kameoka, T. Tanaka, Y. Nojima, S.F. Schlossman, C. Morimoto, Direct association of adenosine deaminase with a T cell activation antigen, CD26, Science 261 (1993) 466–469.

[21] I. De Meester, G. Vanham, L. Kestens, G. Vanhoof, E. Bosmans, P. Gigase, S. Scharpe, Binding of adenosine deaminase to the lymphocyte surface via CD26, Eur. J. Immunol. 24 (1994) 566–570.

[22] R.P. Dong, J. Kameoka, M. Hegen, T. Tanaka, Y. Xu, S.F. Schlossman, C. Morimoto, Characterization of adenosine deaminase binding to human CD26 on T cells and its biologic role in immune response, J. Immunol. 156 (1996) 1349–1355.

[23] M. Martin, J. Huguet, J.J. Centelles, R. Franco, Expression of ecto-adenosine deaminase and CD26 in cells triggered by the T-cell receptor (TCR/CD3) complex: Possible role of adenosine deaminase as costimulatory molecule, J. Immunol. 155 (1995) 4630–4643.

[24] C. Lluis, R. Franco, O. Cordero, Ecto-adenosine deaminase may play a relevant role in the development of the immune system, Immunol. Today 19 (1998) 533–534.

[25] S. Gines, M. Marino, J. Mallol, E.I. Canela, C. Morimoto, C. Callebaut, A. Hovanessian, V. Casado, C. Lluis, R. Franco, Regulation of epithelial and lymphocyte cell adhesion by adenosine deaminase–CD26 interaction, Biochem. J. 361 (2002) 203–209.

[26] A. Valenzuela, J. Blanco, C. Callebaut, E. Jacotot, C. Lluis, A.G. Hovanessian, R. Franco, Adenosine deaminase binding to human CD26 is inhibited by HIV-1 envelope glycoprotein gp120 and viral particles, J. Immunol. 158 (1997) 3721–3729.

[27] R.P. Dong, K. Tachibana, M. Hegen, Y. Munakata, D. Cho, S.F. Schlossman, C. Morimoto, Determination of adenosine deaminase binding domain on CD26 and its immunoregulatory effect on T cell activation, J. Immunol. 159 (1997) 6070–6076.

[28] C.A. Abbott, G.W. McCaughan, M.D. Gorrell, Two highly conserved glutamic acid residues in the predicted β propeller domain of dipeptidyl peptidase IV are required for its enzyme activity, FEBS Lett. 458 (1999) 278–284.

[29] E. Richard, F.X. Arredondo-Vega, I. Santisteban, S.J. Kelly, D.D. Patel, M.S. Hershfield, The binding site of human adenosine deaminase for CD26/dipeptidyl peptidase IV: the Arg142Gln mutation impairs binding to CD26 but does not cause immune deficiency, J. Exp. Med. 192 (2000) 1223–1236.

[30] E. Richard, S.M. Alam, F.X. Arredondo-Vega, D.D. Patel, M.S. Hershfield, Clustered charged amino acids of human adenosine deaminase comprise a functional epitope for binding the adenosine deaminase complexing protein CD26/dipeptidyl peptidase IV, J. Biol. Chem. 277 (2002) 19720–19726.

[31] H.B. Rasmussen, S. Branner, F.C. Wiberg, N. Wagtmann, Crystal structure of human dipeptidyl peptidase IV/CD26 in complex with a substrate analog, Nat. Struct. Biol. 10 (2003) 19–25.

[32] M. Engel, T. Hoffmann, L. Wagner, M. Wermann, U. Heiser, R. Kiefersauer, R. Huber, W. Bode, H.U. Demuth, H. Brandstetter, The crystal structure of dipeptidyl peptidase IV (CD26) reveals its

functional regulation and enzymatic mechanism, Proc. Natl. Acad. Sci. USA 100 (2003) 5063–5068.

[33] K. Ludwig, S. Yan, H. Fan, W. Reutter, C. Böttcher, The 3D structure of rat DPPIV/CD26 as obtained by cryo-TEM and single particle analysis, Biochem. Biophys. Res. Commun. 304 (2003) 73–77.

[34] T. Kinoshita, N. Nishio, I. Nakanishi, A. Sato, T. Fujii, Structure of bovine adenosine deaminase complexed with 6-hydroxy-1,6-dihydropurine riboside, Acta Crystallogr. D 59 (2003) 299–303.

[35] T. Kinoshita, N. Nishio, A. Sato, M. Murata, Crystallization and preliminary analysis of bovine adenosine deaminase, Acta Crystallogr. D 55 (1999) 2031–2032.

[36] W. Wriggers, S. Birmanns, Using situs for flexible and rigid-body fitting of multiresolution single-molecule data, J. Struct. Biol. 133 (2001) 193–202.

[37] J. Dobers, M. Zimmermann-Kordmann, M. Leddermann, T. Schewe, W. Reutter, H. Fan, Expression, purification, and characterization of human dipeptidyl peptidase IV/CD26 in Sf9 insect cells, Protein Expr. Purif. 25 (2002) 527–532.

[38] J. Dobers, S. Grams, W. Reutter, H. Fan, Roles of cysteines in rat dipeptidyl peptidase IV/CD26 in processing and proteolytic activity, Eur. J. Biochem. 267 (2000) 5093–5100.

[39] K. Ludwig, B. Baljinnyam, A. Herrmann, C. Böttcher, The 3D structure of the fusion primed Sendai F-protein determined by electron cryomicroscopy, EMBO J. 22 (2003) 3761–3771.

[40] M. van Heel, Angular reconstitution: a posteriori assignment of projection directions for 3D reconstruction, Ultramicroscopy 21 (1987) 111–123.

[41] M. van Heel, G. Harauz, Biological macromolecules explored by pattern recognition, Scanning Microsc. Suppl. 2 (1988) 295–301.

[42] P.E. Daddona, W.N. Kelley, Human adenosine deaminase binding protein. Assay, purification, and properties, J. Biol. Chem. 253 (1978) 4617–4623.

[43] R.J. Andy, R. Kornfeld, The adenosine deaminase binding protein of human skin fibroblasts is located on the cell surface, J. Biol. Chem. 257 (1982) 7922–7925.

[44] T. Schrader, A. Loidl, G.J. McIntyre, C.M. Zeyen, Single-crystal neutron-diffraction study of the orientational glass state of (NaCN)1–x(KCN)x, Phys. Rev. B 42 (1990) 3711–3718.

[45] K. Kinoshita, J. Furui, H. Nakamura, Identification of protein functions from a molecular surface database, eF-site, J. Struct. Funct. Genomics 2 (2002) 9–22.

[46] T. Kähne, U. Lendeckel, S. Wrenger, K. Neubert, S. Ansorge, D. Reinhold, Dipeptidyl peptidase IV: a cell surface peptidase involved in regulating T cell growth (review), Int. J. Mol. Med. 4 (1999) 3–15.

[47] M.D. Gorrell, C.A. Abbott, T. Kähne, M.T. Levy, W.B. Church, G.W. McCaughan, Relating structure to function in the beta-propeller domain of dipeptidyl peptidase IV. Point mutations that influence adenosine deaminase binding antibody binding, and enzyme activity, Adv. Exp. Med. Biol. 477 (2000) 89–95.

[48] D.K. Wilson, F.B. Rudolph, F.A. Quiocho, Atomic structure of adenosine deaminase complexed with a transition-state analog: understanding catalysis and immunodeficiency mutations, Science 252 (1991) 1278–1284.

[49] C.A. Abbott, G.W. McCaughan, M.T. Levy, W.B. Church, M.D. Gorrell, Binding to human dipeptidyl peptidase IV by adenosine deaminase and antibodies that inhibit ligand binding involves overlapping, discontinuous sites on a predicted beta propeller domain, Eur. J. Biochem. 266 (1999) 798–810.